Numerical Simulation of Pantograph-Catenary Coupling De-icing Based on Orthogonal Experiment Method

WU Lei[1,2*], *XU Mengnan*[1], *ZHANG Huapeng*[1], *WU Wei*[1], *DING Jianming*[3]

1. School of Mechanical Engineering, Southwest Jiaotong University, Chengdu 610031, P. R. China;
2. Key Laboratory of Icing and Anti/De-icing, China Aerodynamics Research and Development Center, Mianyang 621000, P. R. China;
3. State Key Laboratory of Traction Power, Southwest Jiaotong University, Chengdu 610031, P. R. China

(Received 18 March 2023; revised 19 August 2023; accepted 30 August 2023)

Abstract: An investigation was conducted to examine the impact of the operating speed, ice thickness, pantograph head mass, pantograph head stiffness, and pantograph head damping on the de-icing rate. The investigation utilized the orthogonal experimental method and finite element simulation, employing a five-factor four-level orthogonal experimental design. Finite element models (FEM) were utilized to establish models for the ice-coating of the overhead contact system (OCS) and the coupling of the pantograph and catenary (PAC). The accuracy of the FEM was subsequently validated through a comparison between theoretical values and simulation results. The simulation results show that the operating speed and pantograph head mass have a significant impact on the contact force and contact wire lift amount, which in turn affects the de-icing rate. However, the influence of the pantograph head mass becomes less significant when it exceeds 17 kg. The results of the orthogonal experiment suggest that the de-icing rate is primarily influenced by the train speed, pantograph head mass, and ice thickness. The effects of pantograph head stiffness and damping are deemed insignificant. These results can provide references for improving train operation safety and PAC coupling de-icing technology.

Key words: orthogonal experiment; finite element analysis; pantograph and catenary coupling; mechanical de-icing

CLC number: U225 **Document code:** A **Article ID:** 1005-1120(2023)S1-0029-13

0 Introduction

The overhead contact system (OCS) is an important component of the electrified railway system. It provides power to run electric locomotives or trains and ensures safe and stable operations. However, the OCS is vulnerable to meteorological conditions such as strong winds, heavy rain, and snowstorms. These conditions can cause sagging of the contact wire and ice buildup, compromising the safety of train operations and the OCS itself[1-3]. Ice buildup on the OCS can hinder power supply to electrified trains, reduce pantograph's current collection quality, and compromise the safety and reliability of the OCS[4]. Consequently, research on de-icing methods for the OCS is necessary. Currently, the predominant approaches to prevent and de-ice the OCS involve mechanical de-icing, thermal ice-melting, chemical treatment, and online ice prevention technologies. Among these methods, pantograph and catenary (PAC) coupling de-icing can be categorized as a form of mechanical de-icing[5-8]. PAC coupling de-icing is a commonly used method that relies on increasing the contact force between the contact wire and pantograph. This exploits the elastic deformation of the pantograph caused by passing trains, effectively shaking off the ice on the contact wire. This method is simple to operate, applicable to a wide range of scenarios, and has proven to be

*Corresponding author, E-mail address: wuleitpl@163.com.

How to cite this article: WU Lei, XU Mengnan, ZHANG Huapeng, et al. Numerical simulation of pantograph-catenary coupling de-icing based on orthogonal experiment method[J]. Transactions of Nanjing University of Aeronautics and Astronautics, 2023, 40(S1): 29-41.

http://dx.doi.org/10.16356/j.1005-1120.2023.S1.003

effective at de-icing. However, it requires high-performance equipment and skilled technicians. Technicians must accurately control the contact force between the contact wire and pantograph during de-icing operations to prevent damage to the OCS and pantograph[9-10].

Currently, the study of the coupling force de-icing between the pantograph and contact wire is important for reducing accidents caused by ice buildup on the contact wire and improving the safe and stable operation of electrified trains. In addition, it is necessary to research various factors that influence the PAC coupling de-icing in order to improve de-icing efficiency, save resources, and provide theoretical guidance for regulating contact force during pantograph operation. Yu[11] conducted experiments and simulations to study the impact of the PAC coupling force on the ice-coating of OCS, as well as analyzed the effects of train running speed and departure density on de-icing effectiveness. Gao[12] conducted mechanical de-icing experiments on externally loaded OCS and used the "life and death" element technique to simulate the de-icing process of OCS. Yao et al.[13] established a PAC coupling model using the finite element method and compared the effect of current quality on ice thickness on the contact wire using methods such as increased density, uniform load, and composite materials. Furthermore, Kalman[14] studied the effects of span length, transmission line parameters, and ice thickness on de-icing effectiveness under impact loads. For de-icing equipment, copper-based powder sliding pantographs are mainly used in China, although there are cases in the United States where ice knives are used for de-icing, and an Italian company has designed a dedicated ice-breaking pantograph[15].

Currently, the research on PAC coupling de-icing is insufficient. The impact of pantograph parameters on contact wire icing is not yet clear, which presents a gap in knowledge. Therefore, improving the efficiency and economy of PAC coupling de-icing has become a current research focus. To address this gap, it is beneficial to study the impact of various pantograph parameters, such as operating speed, pantograph head mass, and pantograph head stiffness, on contact wire de-icing effects. This knowledge will guide pantograph designs to more accurately and efficiently complete scraping and de-icing operations. This paper aims to address these research gaps by focusing on the simple chain suspension OCS as the research object. First, a simple chain suspension OCS model is constructed. Second, the pantograph is modeled as a binary mass dynamic model coupled with the OCS model. Third, to study the impact of different factors on de-icing effects, an orthogonal experimental method and finite element transient dynamic analysis method are employed. The five factors considered in the study include operating speed, pantograph head mass, pantograph head stiffness, pantograph head damping, and contact wire ice-coating thickness. Finally, the study summarizes the optimal parameter combination for PAC coupling de-icing based on the obtained results.

1 Numerical Simulation Model

This paper aims to analyze the initial state of the contact wire using finite element analysis software. To achieve this, a single-span OCS model and an ice-coating model are built and simulated. In addition, a PAC coupling system is constructed based on the two-element mass dynamic model of the pantograph and a simple chain suspension OCS model. Some approximate assumptions are made in the simulation analysis:

(1) A single anchor segment of the model is taken as the research object, with one end fixed and the other end tensioned.

(2) The contact wire and the tensioning cable are treated as a continuous body with a uniform mass, and the constant tension is considered.

(3) The impact of immediate loads, like wind speed and aerodynamics, is not considered.

(4) The vibration caused by shedding ice on the contact wire is disregarded.

1.1 Icing characteristics and failure criteria

Before conducting analysis on de-icing for

OCS, it is necessary to clarify the characteristics of various types of ice-coating and the corresponding criteria for failure. The OCS ice-coating varies greatly due to differences in geographical and meteorological conditions. Different types of ice-coating require different criteria for failure[16].

The types of ice accretion on the contact wires of OCS can be classified into five categories based on their level of hazard: Snow, hoarfrost, rime, mixed rime, and glaze[17-18]. Glaze, formed from the development of supercooled raindrops, is the most difficult to remove and poses the greatest danger to OCS operation. Glaze ice-coating, with a density greater than 0.9 g/cm^3, exhibits the strongest adhesion force between the crust and the conductor. It is primarily formed when the diameter of supercooled raindrops ranges from 10 μm to 40 μm. Therefore, this paper will analyze the simulation of the PAC coupling de-icing specifically for the glaze icing type. Various factors, such as micro-meteorology, micro-topography, wind speed, air temperature, and the content of supercooled water in the air, affect the ice-coating formation on the contact wires of OCS.

The maximum tensile stress theory can be used as the criterion for determining the failure of the contact wire due to ice-coating, as the adhesive force between the glaze and the wires is strong, and the shear deformation can be neglected when the thickness of the ice-coating is small. Additionally, the ultimate ice shedding strength of the glaze-type ice-coating can be obtained using Eq.(1) for calculating the tensile strength of porous materials with different porosity rates, considering the presence of pores inside the glaze.

$$\sigma_c = \sigma_{c0}\left[\left(\frac{0.38-\phi}{0.38}\right)^{1.85}\left(1-\phi^{\frac{2}{3}}\right)\right]^{\frac{1}{2}} \tag{1}$$

where σ_{c0} represents the tensile strength of the non-porous material; and ϕ the porosity of the material.

Chen et el.[19] provided the ultimate tensile strength for different porosity levels of ice-coating accretion. Assuming a porosity range of 0 to 5% for glazeice-coating, the ultimate tensile strength is determined to be 0.7 MPa[19]. If the stress experienced by an ice-coatingaccretion unit exceeds the ultimate tensile strength, the ice-coating elementis are considered to detach.

1.2 Overhead contact system ice-coating model

A contact wire ice-coating coupling model is established based on the ANSYS finite element software. The initial configuration of the contact wire ice-coating coupling model is determined using the negative sag method. To validate the model, we compare the solutions obtained from theoretical and simulated analyses of the tensioning cable sag for accuracy. The pantograph is represented as a binary mass-dynamics model and is then coupled with the contact wire ice-coating model using the displacement contact method. This step establishes the foundational model for subsequent ice-coating analysis.

1.2.1 Establishment of an OCS ice-coating model

Taking a typical high-speed OCS as an example, the parameters of OCS are shown in Table 1. The span of OCS is 55 m, and the height is 1.6 m. The tensioning cable and contact wire are simulated using the BEAM188 element in ANSYS finite element analysis software, as it is a type of 3D element that can effectively simulate axial compression, bending, and torsion, and can simulate the characteristics of OCS. The suspender, which is relatively thin and undergoes large deformation with a changing cross-sectional area, is simulated using the LINK180 element. To illustrate this, Fig.1 depicts a schematic diagram of a simple chain suspension OCS model.

Table 1 OCS model parameters

Object	Type	Elasticity modulus / Pa	Linear density / (kg•m^{-1})	Tension / kN	Radius / m
Contact wire	CTMH-150	1.21×10^{11}	1.376	30	0.007 2
Tensioning cable	JTMH-120	1.21×10^{11}	1.087	21	0.006 2
Messenger wire	JTMH-120	1.21×10^{11}	0.095	—	0.001 8

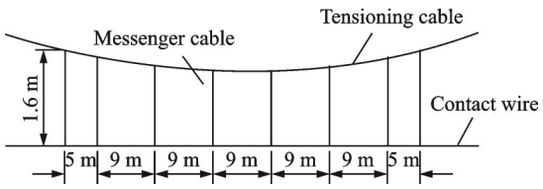

Fig.1 OCS model

BEAM188 element is still used for ice-coating, with an elastic modulus of 10 GPa and a Poisson's ratio of 0.3. The actual contact wire ice-coating is affected by gravity, and the ice-coating cross-section is complex. To better fit the reality, the ANSYS custom beam cross-section function is used to build an eccentric contact wire ice-coating model, as shown in Fig.2, where d is the ice-coating thickness. By coupling, the ice-coating is loaded onto the contact wire model.

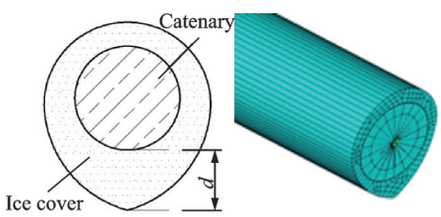

Fig.2 OCS ice-coating model

1.2.2 Contact wire model shape analysis

When conducting finite element analysis on the OCS model, it is necessary to determine the initial shape of the OCS model before de-icing analysis. This is because, in reality, the contact wire is pulled up by the messenger wire, maintaining an approximately horizontal state, while during the analysis, the tensioning cable and the middle part of the contact wire naturally sag under the self-weight load. Thus, the "finding the shape" of the OCS is essential to accurately simulate the real-world behavior in the analysis.

The process of finding the shape of the OCS using the negative sag method is illustrated in Fig.3. Sag refers to the phenomenon of sagging in cable structures. To solve this, the negative sag method is used in this study. The negative sag method applies the reverse displacement caused by the sagging of the contact wire to the contact wire, continuously updating it until the vertical displacement of the contact wire meets the required standards.

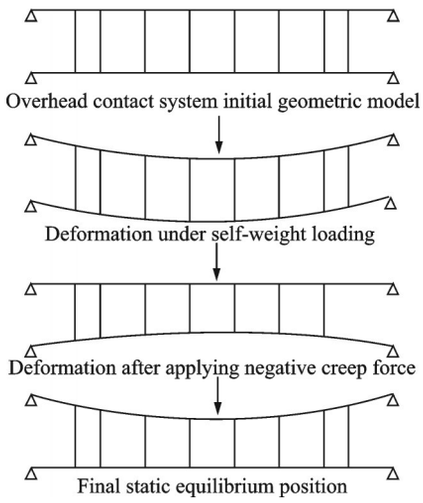

Fig.3 Negative sag method for constructing shape diagrams

The general approach for solving the problem involves the following steps: First, establishing an initial model of OCS; second, applying self-weight load to determine the vertical displacement of the tensioning cable and contact wire considering gravity and horizontal tension; third, the obtained vertical displacement is used to calculate the corresponding negative sag for the contact wire; fourth, the messenger wire length is updated and the model is reconstructed. Typically, this process is repeated 3—5 times until the horizontal static equilibrium position of the contact wire is achieved.

1.2.3 Ice-coating load coupling and solution

By employing an initial shape-finding algorithm based on the OCS model, the initial static shape of OCS is obtained. This is illustrated in Fig.4, which displays the equilibrium position cloud map. The data in the legend indicates the sag of tensioning cable in meters. Negative values in the legend signify vertical sagging towards the ground.

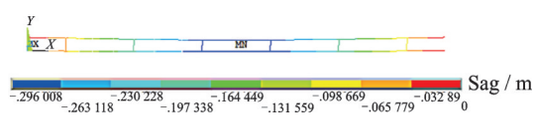

Fig.4 Contact wire static equilibrium position cloud map

Contact wire is in an approximately horizontal state, and the simulation solution for the sag of the tensioning cable is 0.296 m. In the theoretical calculation, taking the suspension point on the left end of

the catenary as the center, a moment is taken on the calculation model, and Eq.(2) is obtained

$$T_{c0} \cdot F_{c0} - T_j \cdot h - \frac{1}{2} q_0 l \cdot \frac{l}{4} + T_j \cdot h = 0 \quad (2)$$

The simplification of Eq.(2) yields calculation Eq.(3) for determining the endurance cable at the approximate contact wire level.

$$F_{c0} = \frac{q_0 l^2}{8 T_{c0}} \quad (3)$$

where F_{c0} represents the sag of the contact wire when it is approximately horizontal under the sag of the tensioning cable; h the height of OCS structure; l the span; T_j the tension of the contact wire; T_{c0} the tension of the tensioning cable when the contact wire is approximately horizontal; q_0 the element synthetic load of the catenary suspension when the contact wire is approximately horizontal.

The OCS and ice-coating models are coupled using the CPINTF command to obtain the OCS ice-coating model, as outlined in the previous sections. A static analysis is then conducted to determine the sag of the tensioning cable after the ice-coating is applied, as illustrated in Fig.5.

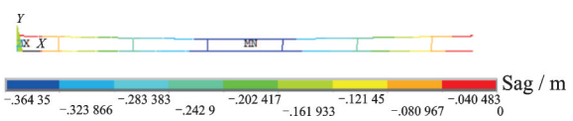

Fig.5 Contact wire ice-coating model static equilibrium position cloud map

After the ice-coating, the sag of the tensioning cable increases by 0.068 m compared to its initial sag. The simulation solution for the tensioning cable sag after ice-coating is 0.364 m. When considering the coupling effect with the OCS and ice coating, the theoretical solution gives a sag of 0.326 m. The error between the simulation and theoretical solutions is a 0.038 m, which meets the model requirements.

1.3 Pantograph-catenary coupling model

During the operation of an electrified train, the pantograph and the OCS are two separate systems with distinct mechanical characteristics. The pantograph experiences an upward lifting force, allowing it to contact the contact wire and consequently integrating the two independent systems[20].

However, in the actual de-icing operation of the train, there is relative displacement between the pantograph's copper-based powder slide and the contact wire in multiple directions, including horizontal, vertical, and lateral movements. This relative displacement makes it challenging to conduct a precise motion force analysis[21]. To simplify the force analysis, the pantograph is categorized as a binary mass-dynamics model, solely focusing on the vertical displacement between the pantograph and the contact wire. It assumes the train maintains a constant speed and moves in a straight line. Fig.6 illustrates the coupling diagram of the pantograph and contact wire, where the equivalent stiffness K_s between PAC is introduced to enable the coupling of pantograph and OCS. The dynamic balance equation of the coupling system is expressed as

$$\boldsymbol{M}\ddot{\boldsymbol{u}} + \boldsymbol{C}\dot{\boldsymbol{u}} + \boldsymbol{K}\boldsymbol{u} = \boldsymbol{F}(t) \quad (4)$$

where $\boldsymbol{M}, \boldsymbol{C}, \boldsymbol{K}$ are the mass matrix, damping matrix, and stiffness matrix of the structure, respectively; $\ddot{\boldsymbol{u}}, \dot{\boldsymbol{u}}, \boldsymbol{u}, \boldsymbol{F}(t)$ the acceleration vector, velocity vector, displacement vector, and load vector, respectively.

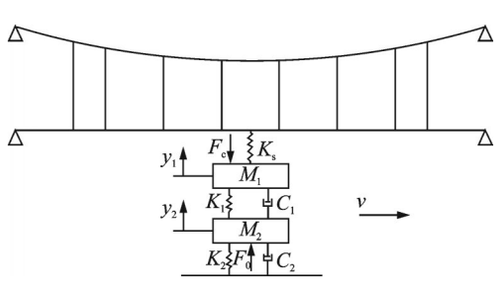

Fig.6 PAC coupling model diagram

When modeling the pantograph using the finite element method, the mass elements of the pantograph head and frame are discretized using the MASS21 element for simulation. The spring damping is simulated using the COMBIN14 element. The contact between the pantograph and the contact wire is established using the CONTA175 and TARGE169 elements[22]. The specific model parameters for the pantograph are presented in Table 2. Furthermore, the mass, stiffness, and damping parameters of the pantograph head are determined through subsequent orthogonal experimental design.

Table 2 Pantograph model parameters

Type	Parameter
Pantograph head mass M_1 / kg	10/13/17/20
Pantograph head rigidity K_1 / (N•m^{-1})	4 000/5 000/ 6 000/7 000
Pantograph head damping C_1 / (N•s•m^{-1})	10/20/30/40
Frame mass M_2 / kg	20
Frame rigidity K_2 / (N•m^{-1})	600
Frame damping C_2 / (N•s•m^{-1})	40

2 Simulation Analysis of Orthogonal Experiment for PAC Coupling De-icing

In order to simplify the analysis difficulty and study the simultaneous effects of these factors, the study aims to investigate the effects of five factors on the de-icing performance of PAC during the de-icing operation. The factors under investigation include the operation speed (V), the pantograph head mass (M), the pantograph head stiffness (K), the pantograph head damping (C), and the ice-coating thickness (T). To achieve this, the study adopts the orthogonal experimental analysis method.

2.1 Orthogonal experimental design

The advantages of orthogonal experimental design are: (1) Balanced factors and uniform distribution of data points, (2) significantly reduced experimental analysis times, (3) corresponding range analysis methods can be used to analyze the experimental results and obtain valuable conclusions[23]. Orthogonal experimental design is a statistical design method to study multiple factors and levels. Its main objective is to explore and determine the factors that influence the experimental results in the minimum number of experiments, in order to further optimize and improve the results[24]. For the five factors affecting deicing effectiveness, four uniform levels were selected for each factor, as shown in Table 3.

An L16(4^5) orthogonal table is used to design 16 sets of simulations for PAC coupling de-icing conditions. From Table 3, it can be seen that the orthogonal experiment involves five factors with four levels. The operation speed is set to 20—80 km/h due to the formation of the contact wire ice-coating, as the current quality of the pantograph deteriorates and the de-icing operation speed should not be too fast. The ice-coating thickness is set to 2—7 mm, as when it reaches around 10 mm, it already affects the normal operation of the electric locomotive. The allowable range for the selection of pantograph parameters is determined during the design and manufacture process[25].

Table 3 PAC de-icing five factors four levels table

Level	V/ (km•h^{-1})	M/kg	K/ (N•m^{-1})	C/ (N•s•m^{-1})	T/mm
1	20	10	4 000	10	2
2	40	13	5 000	20	3
3	60	17	6 000	30	5
4	80	20	7 000	40	7

2.2 Analysis of simulation results for PAC coupling de-icing

Several representative cases were selected according to the simulation results of 16 operating conditions. These cases were then analyzed to determine the contact force, contact wire lift amount, and stress of the ice-coating elements. The impact of various factors on the contact wire de-icing rate was explored, and the accuracy of the model was further validated by comparing the theoretical and simulated values of the contact force.

2.2.1 Contact force

The contact force between the pantograph and the contact wire plays a crucial role in determining the contact quality. A higher contact force implies a better de-icing effect; however, exceeding 200 N can lead to increased friction between the pantograph and the contact wire, resulting in mechanical wear and reduced equipment lifespan[26]. Contact forces lower than 40 N can cause the pantograph to go offline, leading to a decline in current quality and even the occurrence of arc faults that disrupt the equipment's normal operation[27].

The standard deviation of the contact force should not exceed 0.3 times the average contact force, which is calculated using Eq.(5) and reflects the overall contact quality between the pantograph

and the contact wire.

$$F_e = \frac{1}{n}\sum_{i=1}^{n} F_i \tag{5}$$

where F_i represents the ith sampled contact force signal; n the total number of sampled points in this section, and F_e the average contact force.

The standard deviation of contact force, σ, is a crucial indicator to assess overall contact conditions. It reflects the range of contact force fluctuations within the section. It is calculated as

$$\sigma = \sqrt{\frac{1}{n}\sum_{i=1}^{n}(F_i - F_e)^2} \tag{6}$$

The results of the simulation are shown in Table 4, which presents the maximum F_{max}, minimum F_{min}, average F_{avg}, and standard deviation of contact forces for four typical working conditions: 1, 6, 11, and 16. To ensure accuracy, unstable data within the first 5 m at both ends of the contact wire were discarded in the calculations.

Table 4 Contact force statistics under typical operating conditions

No.	V/(km·h^{-1})	M/kg	F_{max}/N	F_{min}/N	F_{avg}/N	σ/N
1	20	10	59.4	37.5	50.0	13.1
6	40	13	69.1	45.3	56.9	13.7
11	60	17	82.6	39.7	59.6	14.8
16	80	20	86.3	43.5	64.9	16.9

The contact forces of the four typical operating conditions, as shown in Table 4 and Fig.7, are within the normal contact range except for the minimum value of the contact force in Condition 1, which is lower than 40 N. This deviation from the normal range can be attributed to the small operating speed and low mass of the pantograph. The standard deviation, which is not greater than $0.3F_e$, further verifies the accuracy of the model. Based on the charts, it can be inferred that there is a general rule: As the operating speed and mass of the pantograph increase, the contact force between the PAC also increases, thus affecting the de-icing rate. It is important to note that a higher contact force leads to a higher de-icing rate.

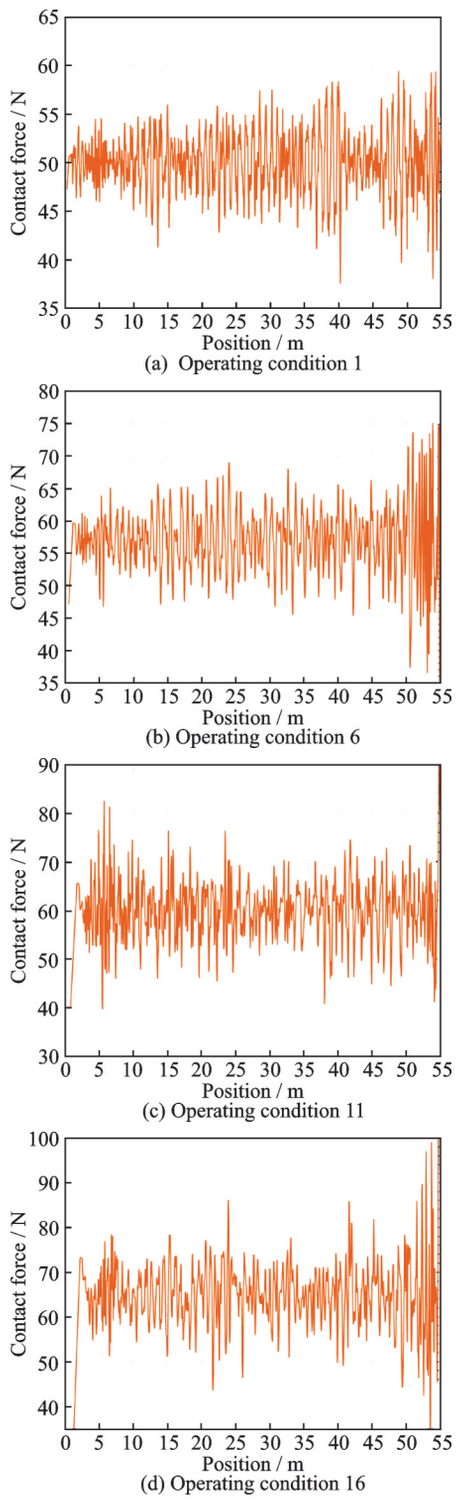

Fig.7 Contact force under typical operating conditions

2.2.2 Contact wire lift amount

When the train starts, the pantograph transmission device applies an upward lifting force to the pantograph, causing it to make contact with the contact wire. Generally, the maximum lift amount of the contact wire should be controlled within

200 mm. As the pantograph completes its lift amount, the contact wire is lifted to a certain degree.

Fig.8 presents the time histories of the longitudinal displacement at the mid-span position, as well as the left and right endpoints, for four different operating conditions. The maximum longitudinal displacement occurs when the pantograph is at this position. With an increase in the operating speed and pantograph mass, the longitudinal displacement at the left and right endpoints demonstrates a less significant change. However, the longitudinal displacement at the mid-span position slightly increases.

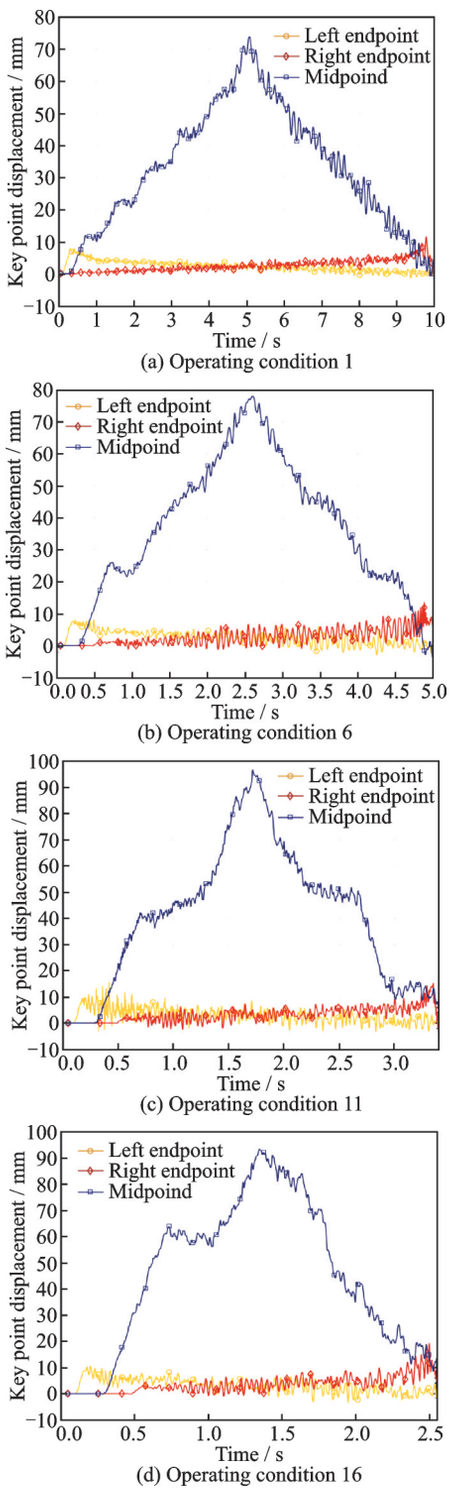

Fig.8 Typical operating condition key point displacement time history

According to Fig.9, the maximum vertical displacement at each position under four operating conditions is extracted to obtain the lift amount. It can be observed that the lift amount under the four typical conditions is within the safe range. Additionally, as the working speed and pantograph quality increase, the lift amount also increases, leading to intensified contact wire vibration and, consequently, an increased de-icing rate.

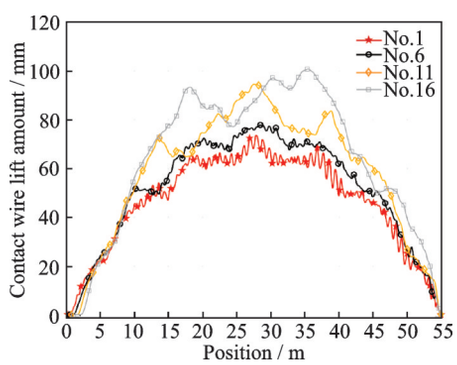

Fig.9 Lift amount under typical operating conditions

2.2.3 Icing elements stress

Changes in the stress of the ice-coating element along the contact wire are induced by mechanical vibrations and contact friction caused by contact force and lift. Ice-coating failure and detachment are determined based on the de-icing criteria mentioned earlier, which states that when the stress of the ice-coating element along the contact wire exceeds 0.7 MPa, ice-coating failure and detachment occur.

Fig.10 presents the stress-time history of the left and right endpoints and the mid-span position under operating condition 8. It reveals that the stress of the ice-coating element experiences constant fluctuations as a result of the oscillation of the contact wire caused by the contact of the pantograph. Consequently, the stress in the ice-coating element fluctuates accordingly. Notably, at the point of contact be-

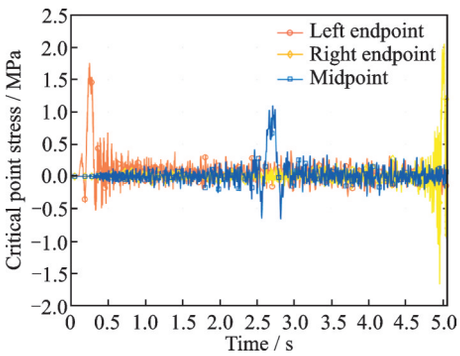

Fig.10 Stress-time history of key points under operating condition 8

tween the pantograph and the contact wire, the stress of the ice-coating element experiences an abrupt change due to the contact force between them. However, as the pantograph moves past this position, the stress at this point returns to minor fluctuations.

The de-icing rate for each operating condition can be calculated from the data in Fig.11 by extracting the maximum stress values of the ice-coating elements on the contact wire under 16 operating conditions and comparing them with the ultimate de-icing stress. This calculation helps in facilitating subsequent de-icing analysis.

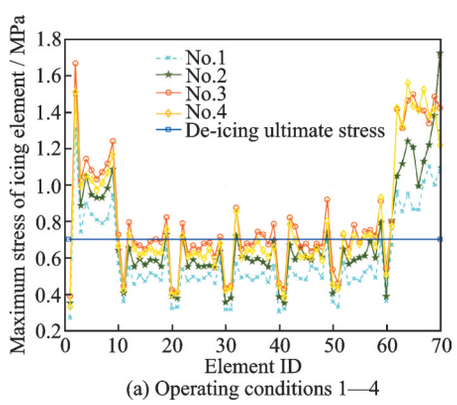

(a) Operating conditions 1—4

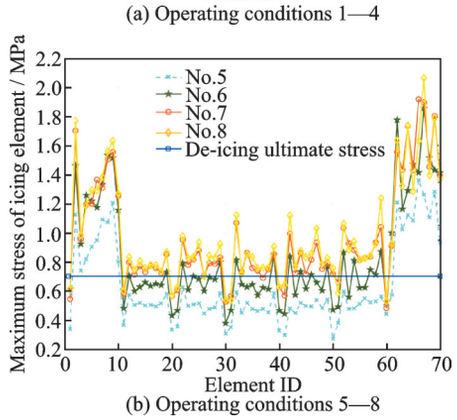

(b) Operating conditions 5—8

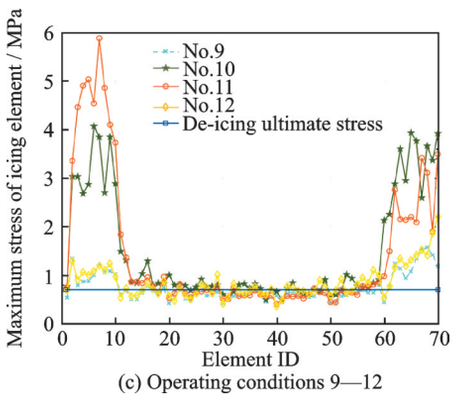

(c) Operating conditions 9—12

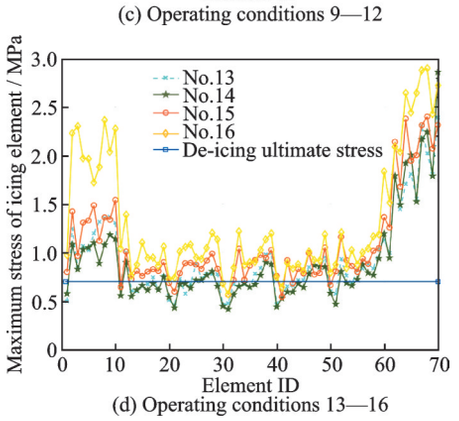

(d) Operating conditions 13—16

Fig.11 Maximum stress of contact wire ice-coating under various operating conditions

2.3 Orthogonal experimental result of range analysis

Methods of range analysis is a statistical method used to analyze the results of orthogonal experiments. It allows the determination of significant factors affecting the experimental results and the optimal combination of levels for these factors. This approach achieves optimal experimental design using the least number of experiments, thereby saving time and costs while enhancing experimental efficiency and accuracy.

In Table 5, K_i ($i = 1, 2, 3, 4$) represents the sum of de-icing rates at the i-th level of a certain factor; $\overline{K_i}$ the average value of K_i, which reflects the influence of different levels of each factor on de-icing rates; R_j ($j = 1, 2, 3, 4$) the range value of each factor, $R_j = \max(K_j) - \min(K_j)$, which reflects the superiority and inferiority of each factor's influence on de-icing rates. A larger R_j value indicates a greater impact of the factor on the de-icing rate.

According to Table 5 and Fig.12, the numerical values indicate that the most significant factor im-

Table 5 Results of orthogonal experiment of PAC coupling de-icing

Test	V / (km•h^{-1})	M / kg	K / (N•m^{-1})	C / (N•s•m^{-1})	T / mm	Deicing-rate / %
No.1	20	10	4 000	10	2	24.3
No.2	20	13	5 000	20	3	32.9
No.3	20	17	6 000	30	5	52.9
No.4	20	20	7 000	40	7	41.4
No.5	40	10	5 000	30	7	25.7
No.6	40	13	4 000	40	5	50.0
No.7	40	17	7 000	10	3	84.3
No.8	40	20	6 000	20	2	85.7
No.9	60	10	6 000	40	3	20.0
No.10	60	13	7 000	30	2	78.6
No.11	60	17	4 000	20	7	52.9
No.12	60	20	5 000	10	5	57.1
No.13	60	10	7 000	20	5	65.7
No.14	60	13	6 000	10	7	55.7
No.15	60	17	5 000	40	2	88.6
No.16	60	20	4 000	30	3	95.7
K_1	151.5	135.7	222.9	221.4	277.2	
K_2	245.7	217.2	204.3	237.2	232.9	
K_3	208.6	278.7	214.3	252.9	225.7	
K_4	305.7	279.9	270.0	200.0	175.7	
$\overline{K_1}$	37.9	33.9	55.7	55.4	69.3	
$\overline{K_2}$	61.4	54.3	51.1	59.3	58.2	
$\overline{K_3}$	52.2	69.7	53.6	63.2	56.4	
$\overline{K_4}$	76.4	70.0	67.5	50.0	43.9	
R_j	38.5	36.1	16.4	13.2	25.4	
Excellent level	V_4	M_4	K_4	C_3	T_1	
Excellent level combination				V_4 M_4 K_4 C_3 T_1		
Primary and secondary order of factors				$V > M > C > K > C$		

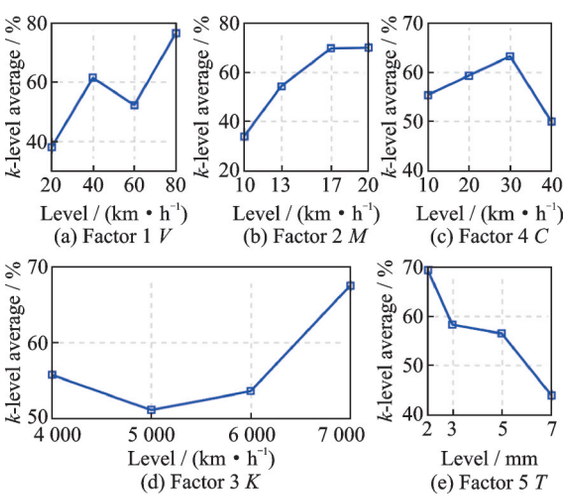

Fig.12 Average plot of factor levels

pacting de-icing rate is Factor 1—Operating speed, followed by Factor 2—Pantograph head mass, Factor 5—Ice thickness, Factor 3—Pantograph head stiffness, and finally Factor 4—Pantograph head Damping. Therefore, the ranking of the five factors, from best to worst, is as follows: Operating speed > pantograph head mass > ice thickness > pantograph head stiffness > pantograph head damping. Based on the optimal levels of each factor, it can be determined that the best de-icing effect is achieved when the operating speed, mass, stiffness, damping of pantograph head, and ice thickness are set at 80 km/h, 20 kg, 7 000 N/m, 30 N·s/m, and 2 mm, respectively. At this optimal level, the de-icing rate is 97.1%, and the stress on the ice-coating element is shown in Fig.13.

To ensure the safe operation of the train, de-icing operations should be conducted before the ice coverage thickness reaches 5 mm. The de-icing operation speed, which is the most critical factor influencing the de-icing rate, should not exceed 80 km/h. Fig.12 suggests that the effect of the pantograph

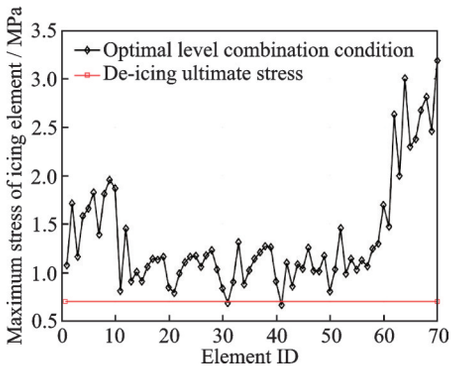

Fig.13 Ice-coating element stress under optimal level operating condition

mass on the de-icing rate gradually plateaus when it exceeds 17 kg. Considering that increasing the mass of the pantograph head will also enhance the running resistance and energy consumption of the operating vehicle, opting for a pantograph head mass of 17 kg is comparatively more efficient and economical. Furthermore, as the ice coverage thickness increases, the de-icing rate decreases rapidly.

3 Discussion and Conclusions

By using orthogonal experimental methods, this article investigates the influence of the PAC coupling effect on the de-icing rate of the contact wire. Numerical simulation methods were used to conduct the study. The study considers various factors, including operation speed, thickness of ice-coating on the contact wire, pantograph head mass, head stiffness, and head damping. The obtained results allow us to draw the following conclusions:

(1) Finite element models of contact wire ice-coating and pantograph-contact wire coupling were established using finite element numerical simulation methods. The validity of the finite element models was assessed by comparing the theoretical values and simulation values of the tensioning cable sag and the standard deviation of the contact force.

(2) Transient dynamic analysis was performed using the displacement contact method based on the established finite element model. The results indicated a significant influence of the operating speed and pantograph head mass on both the contact force and contact wire lift amount. Specifically, an increase in the operating speed and pantograph head mass resulted in higher contact force and lift amount. However, it was observed that the influence of the pantograph head mass reached a plateau when it exceeded 17 kg.

(3) The influencing factors of operating speed, pantograph head mass, stiffness, damping, and contact wire ice-coating thickness were selected for simulation analysis based on orthogonal experimental method. The simulation results were then subjected to range analysis. The de-icing rate was significantly affected by train speed, pantograph head mass, and ice thickness, with train speed being the most significant factor. However, the stiffness and damping of the pantograph head had no significant impact on the de-icing rate.

References

[1] XING Jinhui, CHU Zhenyu, XIE Shaofeng. Research on anti-icing melting technology of high speed railway catenary[J]. Power Capacitor & Reactive Power Compensation, 2022, 43(4): 36-43. (in Chinese)

[2] MACIOLEK T. Methods of reducing the negative influence of weather phenomena, icing in particular, on the operation of an overhead catenary[J]. Rocznik Ochrona Srodowiska, 2016, 32(10): 640-651.

[3] FARZANEH M, CHISHOLM W A. Systems for de-icing overhead power line conductors and ground wires[J]. Techniques for Protecting Overhead Lines in Winter Conditions, 2022, 30(3): 157-194.

[4] SHAO Quandong. Discussion on the method of overhead contact net de-icing[J]. Shanghai Railway Science and Technology, 2012, 23(2): 54-56. (in Chinese)

[5] XIANG Yu, XIE Shaofeng. Study on hybrid anti-melting technology scheme of electric railway catenary[J]. Electric Railway, 2020, 31(2): 15-20. (in Chinese)

[6] LI Qunzhan, GUO Lei, SHU Zeliang, et al. On-line anti-ice technology for catenary of electrified railway[J]. Journal of the China Railway Society, 2013, 43(10): 46-51. (in Chinese)

[7] WANG Y. An online thermal deicing method for urban rail transit catenary[J]. IEEE Transactions on Transportation Electrification. 2021, 194(7): 870-882.

[8] GONG Yansheng, WANG Qiang, HUANG Wenxun, et al. Study on mechanical deicing technology for

catenary[J]. High Speed Railway Technology, 2018, 29(1): 43-47. (in Chinese)

[9] LIN S, SUN X, YU Q, et al. Risk assessment for traction power supply system considering the influence of multiple meteorological factors[J]. IEEE Transactions on Transportation Electrification, 2023, 54(7): 2645-2658.

[10] LIU H, GU X S, TANG W B. Icing and anti-icing of railway contact wires[J]. Reliability and Safety in Railway, 2012, 31(4): 322-342.

[11] YU Wenyang. Analysis of iced catenary and de-icing effect about pantograph-catenary coupling force[D]. Chengdu: Southwest Jiaotong University, 2017. (in Chinese)

[12] GAO Xiaojie. Study on impact of mechanical vibration to catenary icing[D]. Chengdu: Southwest Jiaotong University, 2016. (in Chinese)

[13] YAO Y M, ZHOU N, Mei G, et al. Dynamic analysis of pantograph-catenary system considering ice coating[J]. Shock and Vibration, 2020, 19(1): 145-153.

[14] KALMAN T P. Dynamic behavior of iced overhead cables subjected to mechanical shocks[D]. Huddersfield,Canada: University of Huddersfield, 2005.

[15] LIU Lin. Discussion on icing monitoring and deicing scheme of overhead contact system[D]. Beijing: China Academy of Railway Sciences, 2022. (in Chinese)

[16] LUBOMIR M, CHRISOTO T G. A review of ice and snow risk mitigation and control measures for bridge cables[J]. Cold Regions Science and Technology, 2022, 193(9): 215-229.

[17] FRITJOF N. Modelling anti-icing of railway overhead catenary wires by resistive heating[J]. International Journal of Heat and Mass Transfer. 2019, 143(7): 118-134.

[18] CHAI Hao. Study on the causes, characteristics and simulation of ice cover on power transmission lines in the southern region[D]. Nanjing: Nanjing University of Information Science and Technology, 2022. (in Chinese)

[19] CHEN Kequan, YAN Bo, ZHANG Hongyan, et al. Numerical simulation of de-icing on transmission lines under shock load[J]. Chinese Journal of Applied Mechanics, 2010, 27(4): 761-766,853. (in Chinese)

[20] ZHOU Qun, YANG Jian, SONG Ruigang, et al. Experimental modeling of pantograph and coupled vibration analysis of pantograph[J]. Computer Simulation, 2021, 38(1): 144-149. (in Chinese)

[21] ZHANG W, ZOU D, TAN M, et al. Review of pantograph and catenary interaction[J]. Frontiers of Mechanical Engineering, 2018, 13(6): 311-322.

[22] GREGORI S, TUR M, NADAL E, et al. Fast simulation of the pantograph-catenary dynamic interaction[J]. Finite Elements in Analysis and Design, 2017, 129(7): 1-13.

[23] CHEN M, ZHANG Z B, DENG Q G, et al. Optimization of underfloor air distribution systems for data centers based on orthogonal test method: a case study[J]. Building and Environment, 2023, 23(2): 185-198.

[24] GONG J L. Optimization of a magnetic drive blender orthogonal experiment method and experimental verification[J]. American Journal of Electromagnetics and Applications, 2022, 10(1): 103-119.

[25] ZENG Yutian. Research on the dynamic performance of pantograph-catenary in electrified railway[D]. Nanchang: East China Jiaotong University, 2018. (in Chinese)

[26] YAO Y M, ZHOU D, ZHOU N, et al. A mathematical model for pantograph-catenary interaction[J]. Mathematical and Computer Modelling of Dynamical Systems, 2016, 22(5): 463-474.

[27] NAVIK P, RONNQUIST A, STICHEL S. Variation in predicting pantograph-catenary interaction contact forces, numerical simulations and field measurements[J]. Vehicle System Dynamics, 2017, 55(9): 1265-1282.

Acknowledgements This work was supported by Sichuan Science and Technology Program (No. 2021YFG0194), and the Key Laboratory of Icing and Anti-icing, China Aerodynamics Research and Development Center (No. IADL20210410).

Author Dr. **WU Lei** received his B.S. degree in thermal and power engineering and Ph.D. degree in vehicle application engineering from Southwest Jiaotong University, China in 2005 and 2012, respectively. Since 2012, he has been working at the School of Mechanical Engineering of Southwest Jiaotong University. His research interests include intelligent operation and maintenance of electrified railway, numerical simulation, wheel-rail relationship and rail grinding.

Author contributions Dr. **WU Lei** designed the overall research framework and established a bow-net coupled deicing model. Mr. **XU Mengnan** conducted research and analysis on the pantograph-catenary coupling de-icing model

established and explained the results. Mr. **ZHANG Huapeng** contributed to the background and research status. Mr. **WU Wei** charted the chart. Dr. **DING Jianming** made suggestions on the structure and content of this paper. All authors commented on the manuscript draft and approved the submission.

Competing interests The authors declare no competing inrest.

(Production Editor: ZHANG Bei)

基于正交实验法的弓网耦合除冰数值模拟

吴 磊[1,2], 徐梦楠[1], 张华鹏[1], 吴 蔚[1], 丁建明[3]

(1.西南交通大学机械工程学院,成都 610031,中国; 2.中国空气动力研究与发展中心结冰与防除冰重点实验室,绵阳 621000,中国; 3.西南交通大学牵引动力国家重点实验室,成都 610031,中国)

摘要:基于正交实验方法和有限元仿真方法,设计五因素四水平正交实验表,研究了作业速度、覆冰厚度、弓头质量、弓头刚度以及弓头阻尼对除冰率的影响。建立了接触网-覆冰有限元模型和受电弓-接触网耦合有限元模型,并通过对比理论值和仿真值验证了有限元模型的准确性。仿真结果表明:作业速度和弓头质量对接触力和接触线抬升量影响较大,进而影响除冰率,但弓头质量大于 17 kg 后影响程度趋于平缓。正交实验结果表明:列车运行速度、弓头质量和覆冰厚度是影响除冰率的主要因素,而弓头刚度和阻尼对除冰率影响不显著。这些结果可为提高列车行驶安全性、改善弓网耦合除冰技术提供参考。

关键词:正交试验法;有限元分析;弓网耦合;机械除冰